Geophysical Research Letters®

Measuring Low Plasma Density in the Earth's Equatorial Magnetosphere From Magnetosonic Waves

R. B. Horne[1] [ID], **T. A. Daggitt[1]** [ID], **N. P. Meredith[1]** [ID], **S. A. Glauert[1]** [ID], **X. Liu[2]** [ID], and **L. Chen[2]** [ID]

[1]British Antarctic Survey, Cambridge, UK, [2]Department of Physics, University of Texas at Dallas, Richardson, TX, USA

Abstract The plasma density is one of the most fundamental quantities of any plasma yet measuring it in space is exceptionally difficult when the density is low. Measurements from particle detectors are contaminated by spacecraft photoelectrons and methods using plasma wave emissions are hampered by natural plasma instabilities which dominate the wave spectrum. Here we present a new method which calculates the density from magnetosonic waves near the lower hybrid resonance frequency. The method works most effectively when the ratio of the plasma to cyclotron frequency is $fpe/fce < 3.5$. The method provides a lower bound on the plasma density. Using the new method we show that wave acceleration of electrons to relativistic energies is increased by orders of magnitude. The method enables years of satellite data to be re-analyzed for the Earth and the effectiveness of wave acceleration at the Earth, Jupiter and Saturn to be re-assessed.

Plain Language Summary The electron plasma density is a fundamental quantity of any plasma, but it is very difficult to measure in space using satellites. Satellites charge to different potentials with repel or attract electrons making the true measurement very difficult. The plasma density can be determined from wave oscillations at the plasma frequency, but the waves are difficult to identify as the wave spectrum is often dominated by other much stronger waves. Here we analyze satellite data and show that magnetosonic waves near the lower hybrid resonance frequency can be used to calculate the plasma density. This method provides a lower bound on the density. We show that this lower density leads to much faster electron acceleration by wave-particle interactions, accelerates electrons to much higher energies and increases the electron flux at one MeV by two orders of magnitude or more. The method enables the importance of electron acceleration at the Earth, Jupiter and Saturn to be re-evaluated.

1. Introduction

The plasma density plays a key role in resonant wave-particle interactions responsible for electron pitch angle diffusion and loss from the Earth's radiation belts (e.g., Horne and Thorne (2003); Meredith et al. (2002)). It also controls the upper energy limit of electron acceleration to relativistic energies by wave-particle interactions, and other properties of the plasma, such as the Debye length.

Measuring the plasma density in space using satellites is problematic. Photoelectron emission from a satellite in sunlight contaminates electron flux measurements at energies of a few eV resulting in large uncertainties. Secondary electron emission adds to the uncertainty. Even in sunlight, spacecraft can charge to large negative potentials as high as a few kV (Fennell et al., 2008; Roederer & Fennell, 2009) which repels low energy electrons making accurate measurements very difficult.

Plasma wave emissions at the plasma frequency fpe, or the upper hybrid resonance frequency f_{UHR}, are often used to derive the plasma density, but even this is acknowledged to be problematic when the density is low (Kurth et al., 2015). Figure 1a, taken from the EMFISIS instrument on the Radiation Belt Storm Probes A (RBSP-A) satellite (Kletzing et al., 2013, 2023) illustrates the problem. During the initial part of the event, when the satellite was on an outbound pass within a few degrees of the magnetic equator, f_{UHR} was identified around 100 kHz as indicated by the solid white line. After 19:30 UT there are plasma wave emissions in multiple bands above fce. These are electrostatic electron cyclotron harmonic waves, also known as electron Bernstein waves or $(n + \frac{1}{2})fce$ emissions, although the waves can appear at any frequency inside each harmonic band (Gough et al., 1979; Kennel et al., 1970). These waves are excited by plasma instabilities such as a loss cone or temperature anisotropy in the particle distribution (Ashour-Abdalla & Thorne, 1978; Horne et al., 1981) in frequency bands above fce up to and including f_{UHR} and higher bands. Trying to establish which wave emission corresponds to f_{UHR} is therefore very difficult.
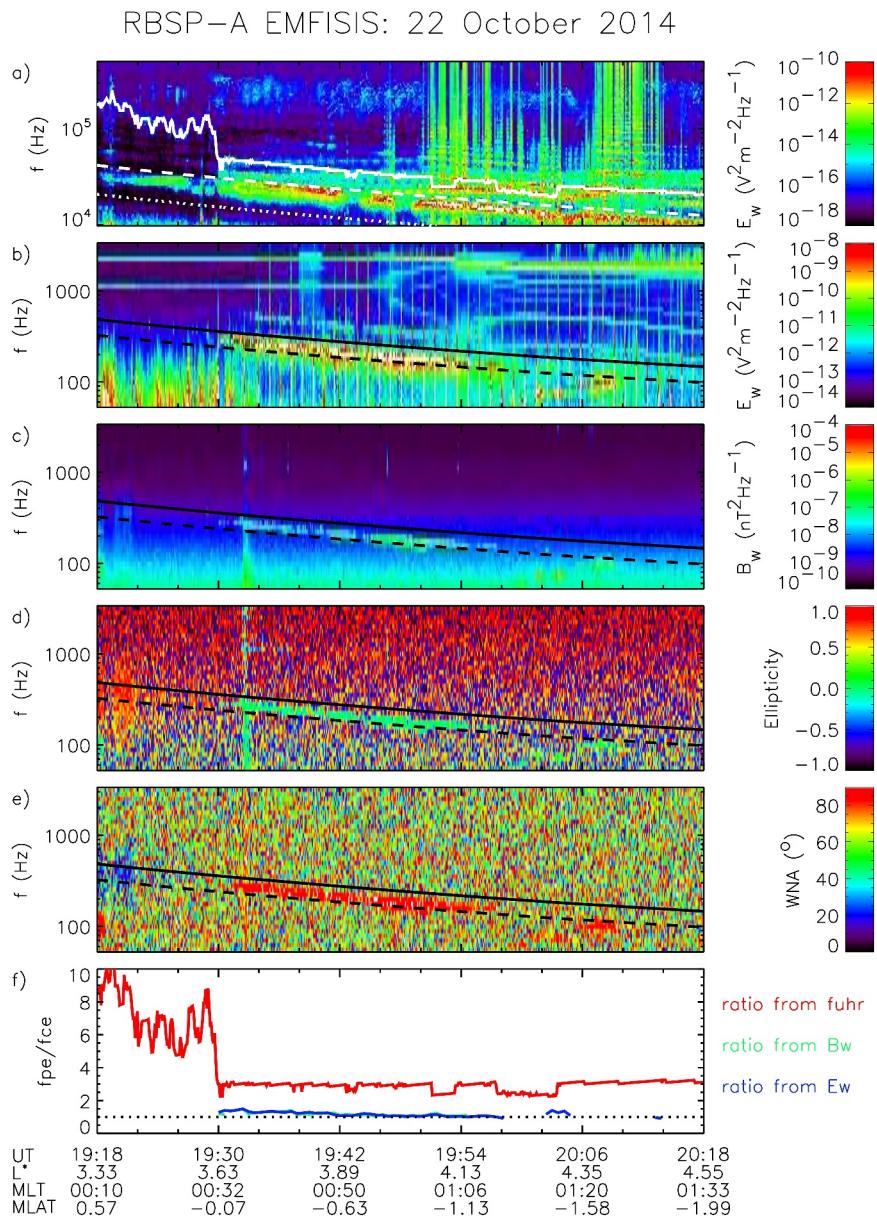
Figure 1. Plasma wave data from the EMFISIS instrument from RBSP-A. (a) Electric field power spectral density above 10 kHz, (b) below 3 kHz, (c) magnetic field power spectral density, (d) ellipticity of the waves (from Santolík et al. (2002)), (e) wave normal angle (from Santolík et al. (2003)), (f) fpe/fce derived from observations of (red) f_{UHR} and f_{LHR} using magnetic (green) and electric (blue) sensors. The white line in 1a is f_{UHR}, the dotted line is fce, and the dashed line is $2fce$. The solid (dashed) line in the other panels is f_{LHR}^{HD} $\left(0.67 f_{LHR}^{HD}\right)$ calculated from the high-density approximation.

Kurth et al. (2015) developed an algorithm to identify f_{UHR} from the most intense band above $\frac{3}{2}fce$ using EMFISIS data. However, they noted several limitations in the method when ECH waves are present, and that this mainly affects the low-density regime. They noted that the $\frac{3}{2}fce$ band is often the most intense, and that if there are no additional cyclotron harmonic bands above this, they hesitate to identify this band as f_{UHR}. They also stated that they hesitate to follow f_{UHR} when the frequency is below 10 kHz due to the spectral resolution of the instrument and that in these cases they leave a gap in the data. If continuum radiation is present, they use the lower frequency cut-off as an indicator of fpe but noted that the cut-off could be due to a plasma density structure at a remote location that prevents propagation to the satellite. Thus, again the local density could be much lower. For example, after 19:30 UT the white line in Figure 1a shows where f_{UHR} has been identified in the second or third band while
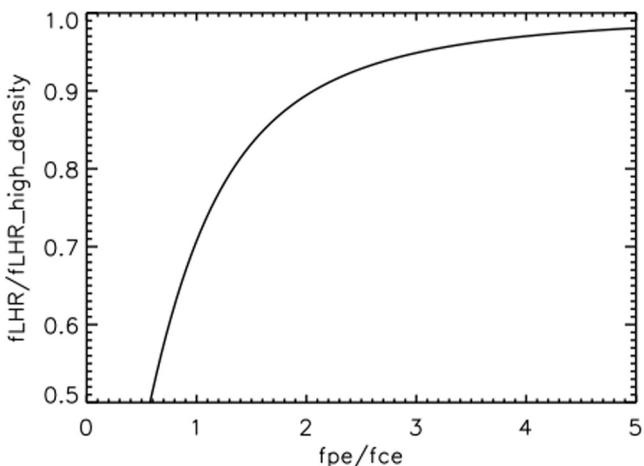
Figure 2. Effects of plasma density on f_{LHR}. Reducing the density reduces f_{LHR} compared to the high density approximation.

the strongest emissions are in the $\frac{3}{2}fce$ band. We note that if ECH waves in the first band had been used to identify f_{UHR}, this would have led to lower values of $fpe/fce \approx 1.4$, and closer to the values we derive later from f_{LHR}. The problem is that we cannot tell if waves in the first band are stronger because they have a longer path length or because they have a lower group velocity associated with the upper hybrid frequency (e.g., see Figure 7 of Horne, Thorne, et al. (2003)). Criteria similar to that of Kurth et al. (2015) have been used to train neural networks (e.g., Zhelavskaya et al. (2016)) and while they may work well for high densities they are likely to suffer the same uncertainty for low density.

Inspection of the RBSP level 4 data shows that fpe/fce is missing for 27% of the mission and that $fpe/fce < 2$ for less than 1% of reported values of fpe/fce. This suggests that despite the best attempts, the data are biased against low densities. Since electron acceleration by wave-particle interactions depends critically on low values of fpe/fce (Allison et al., 2021; Horne, Glauert, & Thorne, 2003) it is important to find a better way of deriving the plasma density particularly for active conditions when electron acceleration is more likely to take place.

2. Waves Near the Lower Hybrid Resonance Frequency

Wave emissions near the lower hybrid resonance frequency f_{LHR} are often observed in the Earth's magnetosphere (e.g., Liu et al. (2021)). Since f_{LHR} depends on both the plasma density and magnetic field here we suggest that waves near f_{LHR} could be used as an alternative way to derive the plasma density in the Earth's radiation belts. This method has been explored for the auroral region (Mozer et al., 1979) and applied to the high latitude/low altitude region of Jupiter (Sulaiman et al., 2021), but here we develop it for the equatorial region of the Earth. For an electron-hydrogen plasma f_{LHR} can be obtained from setting $S = 0$ in the dielectric tensor (Stix, 1992) and $fcH \ll fce$

$$f_{LHR} = \left[\frac{fcefcH(fcefcH + fpe^2)}{(fpe^2 + fce^2)} \right]^{\frac{1}{2}} \tag{1}$$

where fcH is the proton cyclotron frequency. A recent survey using RBSP data found that waves near f_{LHR} are confined to within a few degrees of the magnetic equator and have an occurrence rate of 10% in the inner magnetosphere (Liu et al., 2021). They also found that as AE* increases the waves extend to all magnetic local times inside the plasmapause and are observed outside around dawn. The survey used the plasma density from the upper hybrid frequency, which as discussed above, is not well suited to measuring low plasma density. The waves were identified from four criteria, including that wave electric field spectral density in the range 0.9 and $1.1f_{LHR}$ had to be five times larger than neighboring frequency bands (Liu et al., 2021).

In the high density approximation $f_{LHR}^{HD} = \sqrt{fcefcH}$. However as fpe/fce becomes smaller Figure 2 shows that the reduction in the density reduces f_{LHR}/f_{LHR}^{HD} substantially. The lower limit of f_{LHR} is fcH. By analogy with waves at f_{UHR}, this suggests it may be possible to identify low plasma density from wave emissions near f_{LHR}. Note that the effect is most important for low fpe/fce, the region that is most difficult to identify the density from f_{UHR}. As the wave frequency approaches f_{LHR}^{HD} there is likely to be a large uncertainty in calculating fpe/fce so we restrict the analysis to $f < 0.95f_{LHR}^{HD}$ so that the results are restricted to $fpe/fce < 3.5$.

Figure 1b shows the electric field power spectral density for the same period as in Figure 1a. After 19:30 UT there are strong wave emissions between f_{LHR}^{HD} (solid line) and $0.67f_{LHR}^{HD}$ (dotted line). The magnetic field power spectral density (Figure 1c) shows that these waves are electromagnetic, and that the ellipticity of the waves is close to zero (Figure 1d). Right (left) hand circular polarisation corresponds to 1 (−1) so the ellipticity shows that the waves are linearly polarized. The wave normal angle is strongly aligned close to 90° indicating that these waves are propagating across the background magnetic field with the magnetic field component aligned along the background magnetic field and are thus magnetosonic waves (Horne et al., 2000).
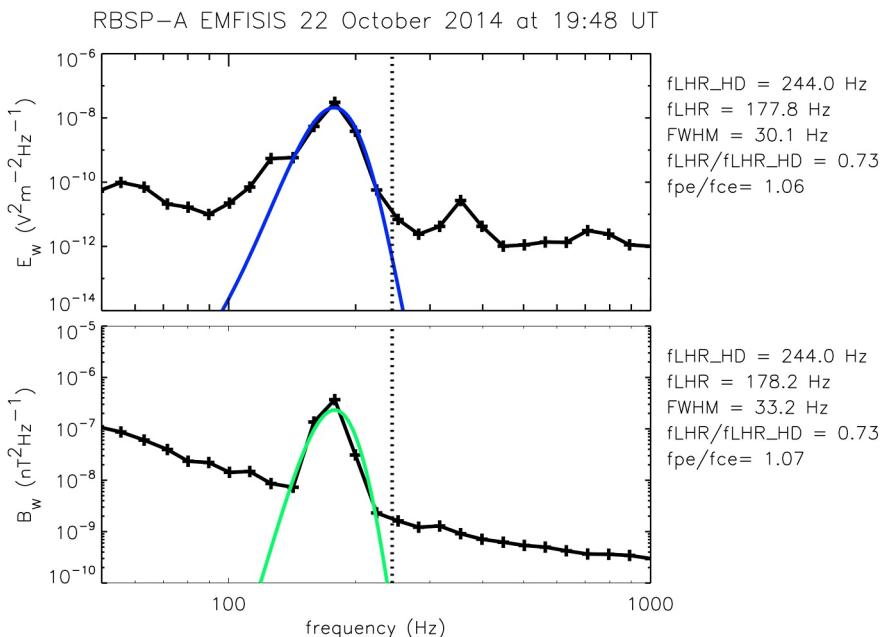
Figure 3. (top) electric and (bottom) magnetic power spectral density from RBSP-A at 19:48 UT on 22 Oct 2014. Gaussian fits were used to derive *fpe/fce*.

By fitting a Gaussian distribution to the electric and magnetic field power spectral density at 19.48 UT (Figure 3) and taking the frequency of the peak we obtain f_{LHR} = 177.8 and 178.2 Hz from which f_{LHR}/f_{LHR}^{HD} = 0.73 and 0.73, and *fpe/fce* = 1.06 and 1.07, respectively. This is much lower than that could be obtained from f_{UHR} in Figure 1a. Note that wave power is enhanced above the background at frequencies just above the peak but below f_{LHR}^{HD}. Therefore, we consider this determination as a lower limit on the plasma density.

Figure 1f shows that *fpe/fce* obtained from f_{LHR} (blue and green) is consistently lower that obtained from f_{UHR} (red line). Before 19:30 UT RBSP-A was in the high-density region where *fpe/fce* cannot be determined from f_{LHR}.

The effects of lower *fpe/fce* on electron acceleration by chorus plasma waves is shown in Figure 4. Above about 300 keV there is a significant increase in electron flux above the initial spectrum (black line). By one MeV the flux is three orders of magnitude higher (red line) using the density determined from f_{LHR} compared to that using f_{UHR} (blue line). Here we have assumed the quasi-linear approximation and used the PADIE code to calculate the diffusion rates (Glauert & Horne, 2005) assuming a band of chorus waves at $L = 4$ propagating along the field line with a Gaussian spread of frequencies with a peak at 0.25 *fce*, width 0.05 *fce*, over a latitude range of 0–6° and an angular distribution peaked in the field aligned direction with a width of $X = \tan \psi = 0.27$ and intensity of 10^{-3} nT^2 (Meredith et al., 2020). The simulation was run to steady state (6.7 hr for *fpe/fce* = 4.4 and 13.1 hr for *fpe/fce* = 1.6, but would be shorter for higher intensity). However, nonlinear effects, which are out of scope here, could be even more important.

3. Discussion

There are a number of factors that could affect the determination of *fpe/fce* from f_{LHR}. In theory ion Bernstein waves that propagate between the harmonics of the proton cyclotron frequency can be excited in multiple harmonic bands up to and above f_{LHR} in a hot plasma (Figure 2, Curtis and Wu (1979)). These waves are analogous to ECH Bernstein waves. They are electrostatic where the *k* vector and wave electric field are aligned so that there is virtually no induced wave magnetic field. As far as we are aware, ion Bernstein waves have not been observed in the magnetosphere near the equatorial region, probably due to electron Landau damping on thermal electrons of a few eV (Ashour-Abdalla & Thorne, 1977). Ion Bernstein waves could add to the electric field component but are excluded here by ensuring the waves are electromagnetic.
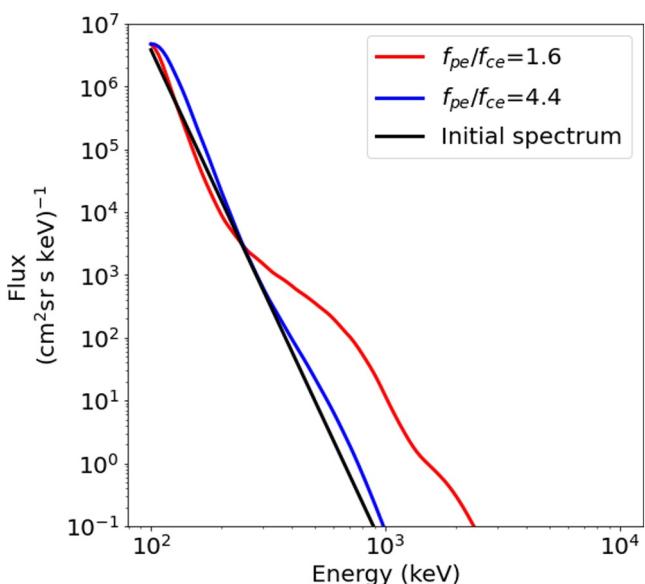
Figure 4. Increase in electron flux due to chorus wave acceleration for *fpe/fce* = 4.4 (blue) and 1.6 (red) at an equatorial pitch angle of 75°. The black line is the initial spectrum.

A second possibility is that magnetosonic waves are only present at frequencies below f_{LHR} leading to an under-estimate of the density. As a rule of thumb, magnetosonic waves can be excited by an ion ring distribution when the ring velocity exceeds the Alfven velocity (Chen et al., 2010, 2011; Horne et al., 2000; Meredith et al., 2008). This usually results in wave growth near the harmonics of the proton cyclotron frequency. Multiple frequency bands are often seen in satellite observations with broader band features at higher frequencies approaching f_{LHR} (e.g., Nemec et al. (2005); Santolík et al. (2002); Boardsen et al. (2014)). Propagation studies show that magnetosonic waves tend to migrate outwards to a region where $f \approx f_{LHR}$ and should form a broad band of waves closely confined to the magnetic equator at frequencies at or just below f_{LHR} (Horne et al., 2000), and this is supported by observations (Liu et al., 2021). Landau damping ensures that the waves are closely confined to the equator. Also, as the group velocity of the waves becomes much smaller for frequencies approaching f_{LHR} the wave energy density should accumulate and become stronger at this frequency as waves from different source regions propagate outwards. However, it is still possible that wave power could peak below f_{LHR} as a result of Landau damping and more surveys are required to test this. As a result, we conclude that the density derived from f_{LHR} should be considered as a lower bound to the density. Magnetosonic waves that propagate inwards would appear at a lower frequency relative to the local f_{LHR}, but since the group velocity is smaller near f_{LHR} the spectrum is more likely to be dominated by outward propagating waves near f_{LHR}, assuming a sufficiently large source region.

Another possibility is that the heavy ion composition could affect the propagation and frequency of magnetosonic waves. The thermal ion composition is very difficult to measure but analysis of electromagnetic ion cyclotron waves outside the plasmapause suggests that the Helium concentration is typically 3%–7% (Anderson et al., 1996). However, ground based measurements of ULF waves suggest that the average ion mass, and hence ion concentration, could be much higher inside the plasmapause near $L = 3$ during active periods (Berube et al., 2005). Heavy ions introduce additional resonances below the helium cyclotron frequency (Horne & Thorne, 1993) but as magnetosonic waves propagate above the proton cyclotron frequency the effects on propagation and growth are likely to be small. However, if the heavy ion fraction is sufficiently large it could reduce f_{LHR} and hence the frequency of magnetosonic waves near f_{LHR}. This would result in a lower determination of *fpe/fce* and hence the density should be considered as a lower limit. Alternatively, if there were a reliable measure of *fpe/fce* available then it may be possible to use waves near f_{LHR} to measure the fraction of heavy ions.

More generally, hot plasma effects remove the resonance at f_{LHR} and in principle wave dispersion enables wave propagation at frequencies above f_{LHR} (e.g., see Figure 2 of Curtis and Wu (1979)). However, waves above f_{LHR} should be heavily Landau damped by thermal electrons (Figure 5, Horne et al. (2000)) and thus again the density derived from f_{LHR} should be considered as a lower bound.

It should be noted that hot plasma effects also remove the resonance at f_{UHR}. The association of intense waves with f_{UHR} assumes that the perpendicular group velocity of ECH waves is in the band containing f_{UHR} and thus the waves grow to larger amplitudes. This is not necessarily the case, since the perpendicular group velocity can be zero in higher harmonic bands and lead to higher amplitude waves in higher bands.

Regions of low plasma density (low *fpe/fce*) are expected just outside the plasmapause during storm times as the plasmapause is eroded and electrons are convected to lower L (Horne, Thorne, Glauert, et al., 2005; Horne, Thorne, Shprits, et al., 2005). The source electron population excites chorus plasma waves which accelerate electrons to relativistic energies and play a major role in forming the Earth's radiation belts. Lower density enables acceleration to higher energies and reaching ultra-relativistic energies (Allison et al., 2021). The method of deriving low plasma density presented here will enable a much better quantification of this process.

At Jupiter, Elliott et al. (2021) used three different types of waves, whistler mode, plasma oscillations and O-mode cut-off, to derive the plasma density in the high latitude low altitude region. There are two main differences to the method proposed here. First, we use magnetosonic waves to identify f_{LHR}, where the magnetosonic waves have

been identified from E and B fields, polarisation and direction of propagation. Second, since magnetosonic waves are largely restricted to the magnetic equator due to propagation effects the method is restricted to the magnetic equatorial region of the magnetosphere. It is complementary.

Our method may also be applicable to the equatorial region at the planets, for example, inside the Io torus at Jupiter where the plasma density drops rapidly and inside the orbit of Enceladus at Saturn. For example, Figure 2a of (Menietti et al., 2017) shows strong ECH waves in the first band detected by Cassini between 20:00 and 22:00 close to the equator but no waves in higher bands, nor continuum radiation. It therefore seems unlikely that the algorithm used to identify f_{UHR} in the Van Allen Probes data would work for this example; indeed, the gap in the white line illustrating f_{UHR} indicates that it has not been possible to identify f_{UHR}. However, more work would be required to determine whether magnetosonic waves are present and could be used in this example.

Wave acceleration of radiation belt electrons has been proposed for Jupiter (Horne et al., 2008) and Saturn (Woodfield et al., 2019). By analogy, if there are regions where *fpe/fce* is lower than that used in modeling studies this could result in more effective acceleration to higher energies.

4. Conclusions

Existing methods of measuring the plasma density either break down or become subject to large uncertainty when *fpe/fce* is low (typically <3). Here we present a new method of calculating a lower bound to the plasma density using magnetosonic waves near f_{LHR}. The method works for *fpe/fce* < 3.5 in regions outside the plasmapause during active periods when the density cannot be easily measured from f_{UHR} due to multiple ECH waves. The method enables low plasma densities to be measured with much greater confidence.

We show that using plasma densities derived from f_{LHR} plasma wave acceleration to ultra-relativistic energies is increased by orders of magnitude. As a result, using densities derived from f_{LHR} should have a profound effect on modeling the Earth's radiation belts, and on forecasting models used for practical applications.

The method enables years of satellite data to be re-analyzed for the Earth and the effectiveness of plasma wave acceleration of electrons at the Earth, Jupiter and Saturn to be re-assessed.

Data Availability Statement

The data used in this paper is level 4 data from the RBSP-A and is available online (https://emfisis.physics.uiowa.edu/data/index).

References

Allison, H. J., Shprits, Y. Y., Zhelavskaya, I. S., Wang, D., & Smirnov, A. G. (2021). Gyroresonant wave-particle interactions with chorus waves during extreme de- pletions of plasma density in the Van Allen radiation belts. *Science Advances*, *7*. https://doi.org/10.1126/sciadv.abc0380

Anderson, B. J., Denton, R. E., Ho, G., Hamilton, D. C., Fuselier, S. A., & Strangeway, R. J. (1996). Observational test of local proton cyclotron instability in the Earth's magnetosphere. *Journal of Geophysical Research*, *101*(A10), 21527–21543. https://doi.org/10.1029/96JA01251

Ashour-Abdalla, M., & Thorne, R. M. (1977). The importance of electrostatic ion-cyclotron instability for quiet-time proton auroral precipitation. *Geophysical Research Letters*, *4*(1), 45–48. https://doi.org/10.1029/GL004i001p00045

Ashour-Abdalla, M., & Thorne, R. M. (1978). Nonconvective and convective electron cyclotron harmonic instabilities. *Journal of Geophysical Research*, *83*(A4), 1531–1543. https://doi.org/10.1029/JA083iA04p01531

Berube, D., Moldwin, M. B., Fung, S. F., & Green, J. L. (2005). A plasmaspheric mass density model and constraints on its heavy ion concentration. *Journal of Geophysical Research*, *110*(A04212). https://doi.org/10.1029/2004JA010684

Boardsen, S. A., Hospodarsky, G. B., Kletzing, C. A., Pfaff, R. F., Kurth, W. S., Wygant, J. R., & MacDonald, E. A. (2014). Van allen probe observations of periodic rising frequencies of the fast magnetosonic mode. *Geophysical Research Letters*, *41*(23), 8161–8168. https://doi.org/10.1002/2014GL062020

Chen, L., Thorne, R. M., Jordanova, V. K., & Horne, R. B. (2010). Global simulation of magnetosonic wave instability in the storm time magnetosphere. *Journal of Geophysical Research*, *115*(A11222). https://doi.org/10.1029/2010JA015707

Chen, L., Thorne, R. M., Jordanova, V. K., Thomsen, M. F., & Horne, R. B. (2011). Magnetosonic wave instability analysis for proton ring distributions observed by the LANL magnetospheric plasma analyzer. *Journal of Geophysical Research*, *116*(A03223). https://doi.org/10.1029/2010JA016068

Curtis, S. A., & Wu, C. S. (1979). Gyroharmonic emissions induced by energetic ions in the equatorial plasmasphere. *Journal of Geophysical Research*, *84*(A6), 2597–2607. https://doi.org/10.1029/JA084iA06p02597

Elliott, S. S., Sulaiman, A. H., Kurth, W. S., Faden, J., Allegrini, F., Valek, P., et al. (2021). The high-latitude extension of jupiter's io torus: Electron densities measured by juno waves. *Journal of Geophysical Research: Space Physics*, *126*(8), e2021JA029195. https://doi.org/10.1029/2021JA029195

Fennell, J. F., Roederer, J. L., Berg, G. A., & Olsen, R. K. (2008). HEO satellite frame and differential charging and SCATHA low-level frame charging. *IEEE Transactions on Plasma Science*, *36*(5), 2271–2279. https://doi.org/10.1109/TPS.2008.2003441

Glauert, S. A., & Horne, R. B. (2005). Calculation of pitch angle and energy diffusion coefficients with the PADIE code. *J. Geophys. Res.Space Physics*, *110*(A04206), 1–15. https://doi.org/10.1029/2004JA010851

Gough, M. P., Christiansen, P. J., Martelli, G., & Gershuny, E. J. (1979). Interaction of electrostatic waves with warm electrons at the geomagnetic equator. *Nature*, *279*(5713), 515–517. https://doi.org/10.1038/279515a0

Horne, R. B., Christiansen, P. J., Gough, M. P., Rönnmark, K., Johnson, J. F. E., Sojka, J., & Wrenn, G. L. (1981). Amplitude variations of electron cyclotron harmonic waves. *Nature*, *294*(5839), 338–340. https://doi.org/10.1038/294338a0

Horne, R. B., Glauert, S. A., & Thorne, R. M. (2003). Resonant diffusion of radiation belt electrons by whistler-mode chorus. *Geophysical Research Letters*, *30*(9), 1493. https://doi.org/10.1029/2003GL016973

Horne, R. B., & Thorne, R. M. (1993). On the preferred source location for the convective amplification of ion cyclotron waves. *Journal of Geophysical Research*, *98*(A6), 9233–9247. https://doi.org/10.1029/92JA02972

Horne, R. B., & Thorne, R. M. (2003). Relativistic electron acceleration and precipitation during resonant interactions with whistler-mode chorus. *Geophysical Research Letters*, *30*(9), 1493. https://doi.org/10.1029/2003GL016973

Horne, R. B., Thorne, R. M., Glauert, S. A., Albert, J. M., Meredith, N. P., & Anderson, R. R. (2005). Timescale for radiation belt electron acceleration by whistler mode chorus waves. *Journal of Geophysical Research*, *110*(A3), A03225. https://doi.org/10.1029/2004JA010811

Horne, R. B., Thorne, R. M., Glauert, S. A., Menietti, J. D., Shprits, Y. Y., & Gurnett, D. A. (2008). Gyro-resonant electron acceleration at Jupiter. *Nature Physics*, *4*, 301–304. https://doi.org/10.1038/nphys897

Horne, R. B., Thorne, R. M., Meredith, N. P., & Anderson, R. R. (2003). Diffuse auroral electron scattering by electron cyclotron harmonic and whistler mode waves during an isolated substorm. *Journal of Geophysical Research*, *108*(A7). https://doi.org/10.1029/2002JA009736

Horne, R. B., Thorne, R. M., Shprits, Y. Y., Meredith, N. P., Glauert, S. A., Smith, A. J., et al. (2005). Wave acceleration of electrons in the Van Allen radiation belts. *Nature*, *437*(7056), 227–230. https://doi.org/10.1038/nature03939

Horne, R. B., Wheeler, G., & Alleyne, H. S. C. K. (2000). Proton and electron heating by radially propagating fast magnetosonic waves. *Journal of Geophysical Research*, *105*(A12), 27597–27610. https://doi.org/10.1029/2000JA000018

Kennel, C. F., Scarf, F. L., Fredricks, R. W., McGehee, J. H., & Coroniti, F. V. (1970). Vlf electric field observations in the magnetosphere. *Journal of Geophysical Research*, *75*(31), 6136–6152. https://doi.org/10.1029/JA075i031p06136

Kletzing, C. A., Bortnik, J., Hospodarsky, G., Kurth, W. S., Santolik, O., Smith, C. W., et al. (2023). The electric and magnetic fields instrument suite and integrated science (EMFISIS): Science, data, and usage best practices. *Space Science Reviews*, *219*(4), 28. https://doi.org/10.1007/s11214-023-00973-z

Kletzing, C. A., Kurth, W. S., Acuna, M., MacDowall, R. J., Torbert, R. B., Averkamp, T., et al. (2013). The electric and magnetic field instrument suite and integrated science (EMFISIS) on RBSP. *Space Science Reviews*, *179*(1–4), 121–181. https://doi.org/10.1007/s11214-013-9993-6

Kurth, W. S., Pascuale, S. D., Faden, J. B., Kletzing, C. A., Hospodarsky, G. B., Thaller, S., & Wygant, J. R. (2015). Electron densities inferred from plasma wave spectra obtained by the waves instrument on Van Allen Probes. *Journal of Geophysical Research: Space Physics*, *120*(2), 904–914. https://doi.org/10.1002/2014JA020857

Liu, X., Chen, L., & Ma, Q. (2021). A statistical study of lower hybrid waves in the earth's magnetosphere by Van Allen Probes. *Geophysical Research Letters*, *48*(10), e2021GL093168. https://doi.org/10.1029/2021GL093168

Menietti, J. D., Averkamp, T. F., Kurth, W. S., Ye, S.-Y., Gurnett, D. A., & Cecconi, B. (2017). Survey of saturn electrostatic cyclotron harmonic wave intensity. *Journal of Geophysical Research: Space Physics*, *122*(8), 8214–8227. https://doi.org/10.1002/2017JA023929

Meredith, N. P., Horne, R. B., & Anderson, R. R. (2008). Survey of magnetosonic waves and proton ring distributions in the Earths inner magnetosphere. *Journal of Geophysical Research*, *113*(A6), A06213. https://doi.org/10.1029/2007JA012975

Meredith, N. P., Horne, R. B., Shen, X.-C., Li, W., & Bortnik, J. (2020). Global model of whistler mode chorus in the near-equatorial region ($|\lambda_m| <$ 18°). *Geophysical Research Letters*, *47*(11), e2020GL087311. https://doi.org/10.1029/2020GL087311

Meredith, N. P., Horne, R. B., Summers, D., Thorne, R. M., Iles, R. H. A., Heynderickx, D., & Anderson, R. R. (2002). Evidence for acceleration of outer zone electrons to relativistic energies by whistler mode chorus. *Annals of Geophysics*, *20*(7), 967–979. https://doi.org/10.5194/angeo-20-967-2002

Mozer, F. S., Cattell, C. A., Temerin, M., Torbert, R. B., Glinski, S. V., Waldorf, M., & Wygant, J. (1979). The dc and ac electric field, plasma density, plasma temperature and field-aligned current experiments on the S3-3 satellite. *Journal of Geophysical Research*, *84*(A10), 5875–5884. https://doi.org/10.1029/JA084iA10p05875

Nemec, F., Santolík, O., Gereova, K., Macusova, E., de Conchy, Y., & Cornilleau-Wehrlin, N. (2005). Initial results of a survey of equatorial noise emissions observed by the Cluster spacecraft. *Planetary and Space Science*, *53*(1–3), 291–298. https://doi.org/10.1016/j.pss.2004.09.055

Roederer, J. L., & Fennell, J. F. (2009). Differential charging of satellite surface materials. *IEEE Transactions on Plasma Science*, *37*(1), 281–289. https://doi.org/10.1109/TPS.2008.2004765

Santolík, O., Pickett, J. S., Gurnett, D. A., Maksimovic, M., & Cornilleau-Wehrlin, N. (2002). Spatiotemporal variability and propagation of equatorial noise observed by Cluster. *Journal of Geophysical Research*, *107*(A12), 1495. https://doi.org/10.1029/2001JA009159

Santolík, O., Pickett, J. S., Gurnett, D. A., & Storey, L. R. O. (2002). Magnetic component of narrowband ion cyclotron waves in the auroral zone. *Journal of Geophysical Research*, *107*(A12). https://doi.org/10.1029/2001JA000146

Santolík, O., Pickett, J. S., Gurnett, D. A., & Storey, L. R. O. (2003). Singular value decomposition methods for wave propagation analysis. *Radio Science*, *38*(1). https://doi.org/10.1029/2000RS002523

Stix, T. H. (1992). *Waves in plasmas*. Springer. Retrieved from https://www.springer.com/gp/book/9780883188590

Sulaiman, A. H., Elliott, S. S., Kurth, W. S., Faden, J. B., Hospodarsky, G. B., & Menietti, J. D. (2021). Inferring jovian electron densities using plasma wave spectra obtained by the juno/waves instrument. *Journal of Geophysical Research: Space Physics*, *126*(8). https://doi.org/10.1029/2021JA029263

Woodfield, E. E., Glauert, S. A., Menietti, J. D., Averkamp, T. F., Horne, R. B., & Shprits, Y. Y. (2019). Rapid electron acceleration in low-density regions of saturn's radiation belt by whistler mode chorus waves. *Geophysical Research Letters*, *46*(13), 7191–7198. https://doi.org/10.1029/2019GL083071

Zhelavskaya, I. S., Spasojevic, M., Shprits, Y. Y., & Kurth, W. S. (2016). Automated determination of electron density from electric field measurements on the Van Allen probes spacecraft. *Journal of Geophysical Research: Space Physics*, *121*(5), 4611–4625. https://doi.org/10.5880/GFZ.2.8.2020.002